Journal of Research and Applications in Mechanical Engineering
ISSN: 2229-2152 (Print); 2697-424x (Online)
(2024) Vol. 12, No. 2, Paper No. JRAME-24-12-022
[DOI: 10.14456/jrame.2024.22]

Research Article

Static Bending Test of a Carbon Fiber Posterior Leaf Spring Ankle Foot Orthoses (PLS-AFOs)

P. Akarasereenont
A. Wisessint*
Department of Mechanical Engineering, Faculty of Engineering, Kasetsart University, Bangkok, 10900, Thailand

Received 27 September 2023
Revised 9 December 2023
Accepted 19 December 2023

Abstract:
Drop foot is a condition that limits the ability to move the foot upward, which can impair walking. Carbon fiber ankle-foot orthoses (AFOs) are commonly used to assist people with drop foot, but they can be expensive and difficult to obtain. This study investigated the use of 3D printing to create carbon fiber posterior leaf spring AFOs (PLS-AFOs). The foot part or Heel support component of PLS-AFOs were printed using carbon fiber and polylactic acid (PLA) filaments. The strength, weight, and load-displacement relationship of the PLS-AFOs were compared. The results showed that PLS-AFOs made from carbon fiber were stronger, and had a better load-displacement relationship than those made from PLA. This suggests that 3D printing can be used to create affordable and accessible carbon fiber PLS-AFOs. The findings of this study will be used to design a new generation of PLS-AFOs that are stronger, and more affordable than traditional AFOs, making them more accessible to people with drop foot.

Keywords: *Ankle Foot Orthosis, Foot drop, Carbon fiber PLS-AFO, Static bending test*

1. Introduction

Foot drop is a condition observed in patients who are unable to dorsiflex their foot, resulting in an altered gait cycle compared to normal walking. The flexible Ankle-Foot Orthosis (AFO) has been designed to help align foot movements with the optimal biomechanics of the gait cycle using the elastic material Polypropylene (PP) [1]. One specific type of Flexible AFO is the posterior leaf spring AFO (PLS-AFO), which addresses challenges in AFO fabrication by separating the posterior leaf spring and heel support components. This division enhances flexibility and load-bearing capabilities, offering an innovative solution for improved foot movement [2].

Fused Deposition Modeling (FDM) is a technology applicable to create AFOs, offering the utilization of a diverse array of materials [3]. Among the material choices, Polylactic acid (PLA) stands out as a commonly preferred option in 3D printing. Its popularity is not only attributed to its user-friendly printing characteristics but also to its significant cost advantage when compared to other available materials. The affordability of PLA is especially crucial in AFO design, ensuring greater accessibility for patients to these essential devices.

Carbon Fiber Reinforced Polymer (CFRP) is a composite material that involves the combination of carbon fiber and polymer, resulting in enhanced material properties [4]. Various types of CFRP filaments, including PLA-CF, PETG-CF, PA-CF, and ABS-CF are employed to introduce improved mechanical property [5]. Among these options, PETG-CF is considered the most cost-effective and readily available choice for this research applications. The parameters

* Corresponding author: A. Wisessint
E-mail address: fengapw@ku.ac.th

for printing each material vary due to differences in their properties and melting points [6]. Specifically, factors such as printing speed and extruder temperature are crucial. If these values are excessively high or low, they can influence the mechanical properties of the filament [7, 8]. This research explores the application of CFRP, produced through FDM, in PLS-AFO design, an area with relatively limited prior exploration [9]. The study aims to compare CFRP's properties with the commonly used PLA material. It involves material property evaluation through ASTM D790-standard Three-Point bending tests and tests on the heel support component of PLS-AFO, with the goal of advancing future AFO designs.

2. Materials and Methods

This study will test and compare the capabilities and properties of PLA and PETG-CF materials. AFO models will be designed in SolidWorks 2020 CAD software and printed using a Prusa MK4 3D printer. The aim is to control printing parameters as closely as possible under similar conditions for each material [10]. Each polymer type will have distinct parameter values, which will be detailed in Table 1 for the experiments.

Table 1: Details of printing parameter.

Material	Printing Parameter						
	Filament diameter (mm)	**Nozzle diameter (mm)**	**Printing speed (mm/s)**	**Layer height (mm)**	**Retraction Speed (mm/s)**	**Extruder temperature (°C)**	**Bed temperature (°C)**
PLA	1.75	0.4	45	0.2	50	215	60
PETG-CF						235	80

2.1 3D Printing Preparation

The printing settings in Table 1 employ a 1.75 mm filament, with PLA at 215 °C and PETG-CF at 235 °C. Specimens base on ASTM D790 standards, measuring 127×12.7×3.2 mm^3, with 100 % infill for the AFO model. The AFO used in testing specifically involves the Heel Support section. It's devised to wear with the patient's shoe, ensuring no direct contact with the skin. This design includes force-receiving points at both ends and an additional gripping shaft, enhancing the device's stability during testing. The heel support section, designed for bearing foot weight, uses a 60 % infill. PETG-CF parameters align with 3DD Digital Fabrication recommendations. Specimens follow the format in Fig. 1, and the heel support model is presented in Figs. 2 and 3.

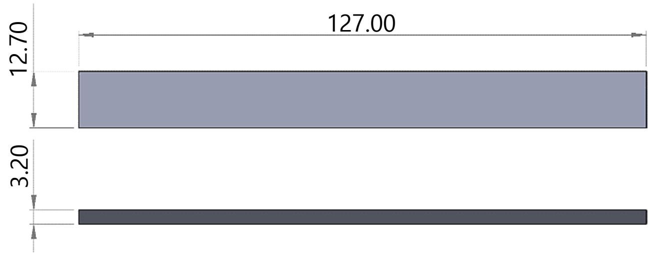

(a)

(b)

Fig. 1. Illustration of (a) Design of the 3point bending specimen according to ASTM D790 and (b) Two difference material from PLA and PETG-CF.

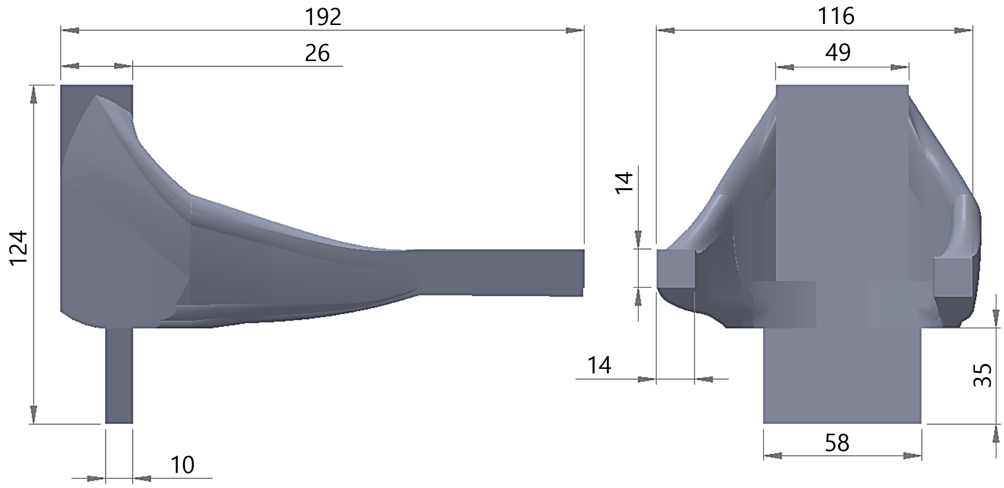

Fig. 2. The design of the AFO model, specifically for the heel support component of the PLS-AFO.

AFOs have been adapted for facilitate attachment to the bending test machine using a 35 mm long, 10 mm thick plate, as shown in Fig. 2. The components of the AFOs model comprise three parts the flexible rod which serves as a posterior leaf spring, the calf support used for banding the patient calf and the heel support that attached to the shoe, as depicted in Fig. 3. In the testing phase, only the heel support component will be utilized.

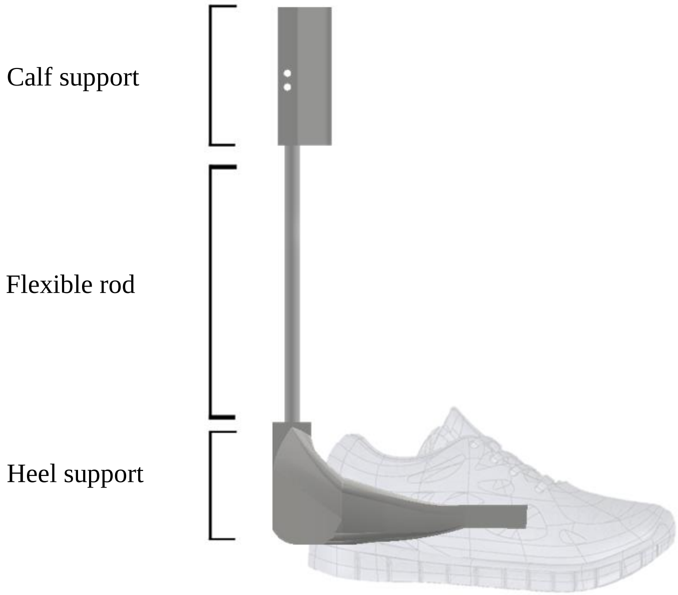

Fig. 3. The components of the designed AFO model consist of three parts.

2.2 Bending Test

2.2.1 Three-Point Bending Test

Specimens, following ASTM D790 standards, were tested using the Instron Electropuls E3000 machine. A 10 mm diameter support and loading nose were positioned through the center, with a testing speed set at 1.37 mm/min, adhering to standard protocols. Initial testing resulted in specimen fractures, prompting an extension of the testing range to 15 mm. Notably, both materials underwent testing under identical conditions to ensure consistency and reliability. Each material was tested with a total of five samples, ensuring a comprehensive evaluation of their mechanical properties. Additionally, the span distance was set to 51.2 mm in accordance with the specifications outlined in Fig. 4.

The applied load during the compression test can be used to calculate the flexural stress and flexural strain in the surface according to Eq. (1) and (2).

$$\sigma_f = 3PL/2bd^3 \tag{1}$$

P represents the load applied during compression. L, b, and d stand for the span, width, and thickness of the specimen, respectively.

$$\varepsilon_f = 6Dd/L^2 \tag{2}$$

Where D is deflection range of loading nose. Equation (1) and (2) can be utilized to calculate the Young's modulus of elasticity (E) using the tangent modulus method, as described in Eq. (3).

$$E_t = L^3m/4bd^3 \tag{3}$$

Where m denotes the slope calculated within the deflection at 0.5 mm to 2.5 mm.

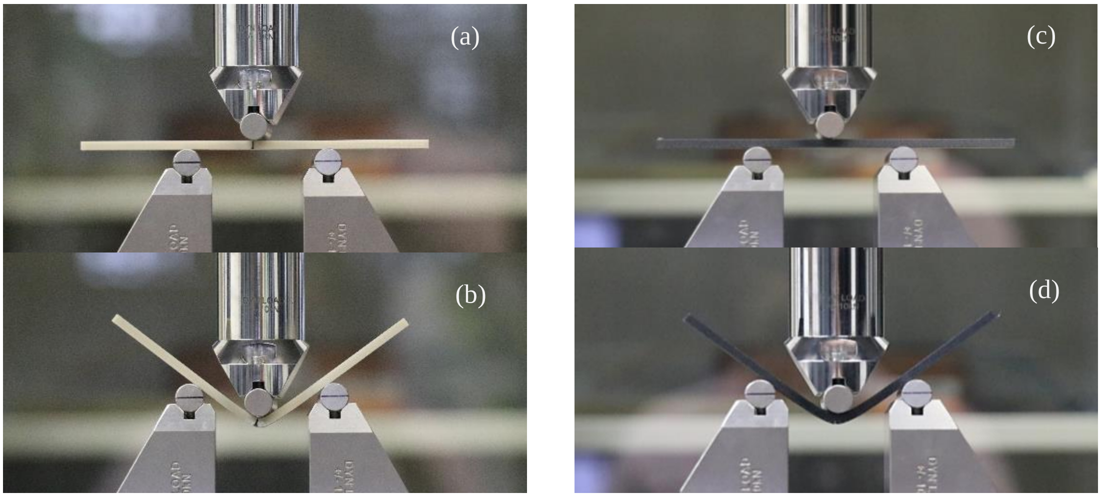

Fig. 4. Illustration of (a) The PLA specimen before compression testing, (b) The PLA specimen after undergoing a 15 mm compression, (c) The PETG-CF specimen before compression testing, (d) The PETG-CF specimen after undergoing a 15 mm compression.

2.2.2 AFO Heel Support Bending Test

The heel support component of the AFO model was subjected to compression testing using the Instron 8801 machine. This involved a reverse direction of the machine to observe the material's recovery post-fracture [11]. Compression was applied over a 45 mm span, utilizing a 10 mm diameter compression head, at a compression speed of 0.1 mm/s. This compression occurred 20 mm from the end of the AFO. The plate attached to the AFO is clamped using grips, applying a hydraulic pressure of approximately 30 bar, equivalent to a gripping force of 20 kN, as illustrated in Fig. 5.

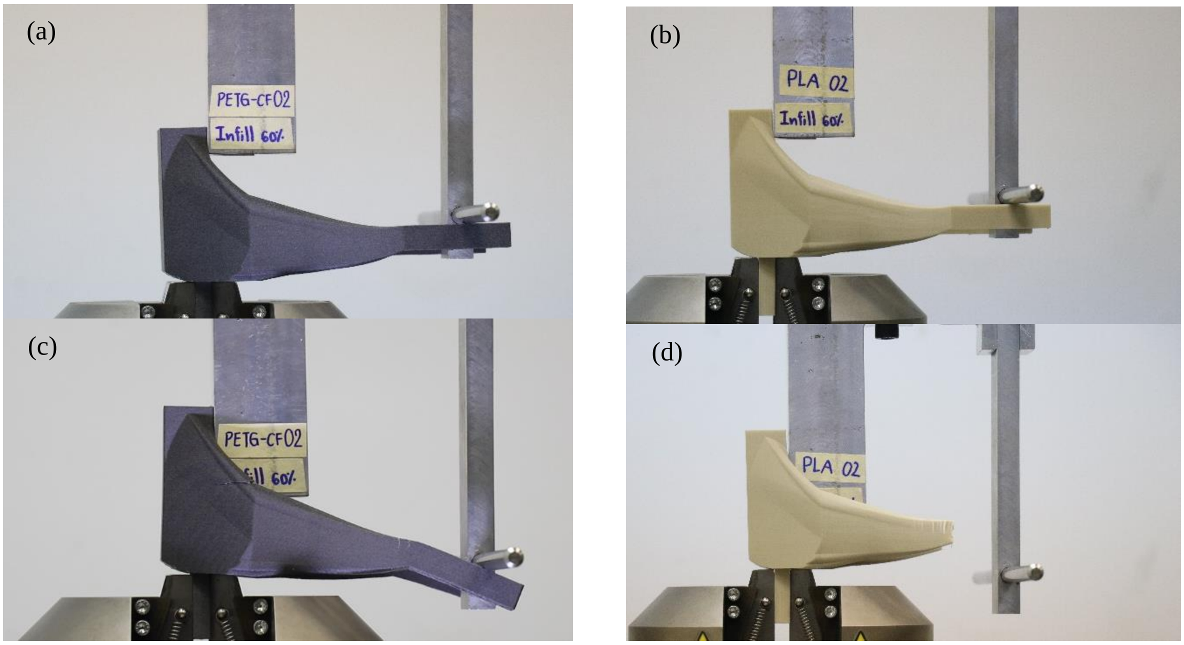

Fig. 5. Illustration of (a) AFO PETG-CF before compression, (b) AFO PLA before compression, (c) AFO PETG-CF after compression and before fracture, (d) AFO PLA after compression and fracture occurrence.

3. Results

3.1 Three Points Bending Test

All five specimens were compressed until a 5% strain, following ASTM D790 standards. This resulted in permanent deformation of both PLA and PETG-CF, as shown in Fig. 6. Material properties obtained from the testing, presented in Table 2, indicate Ultimate Stress and Young's Modulus of Elasticity for PLA and PETG-CF. Notably, PETG-CF demonstrates higher Ultimate Stress with 7% but lower Modulus of Elasticity with 7% compared to PLA, signifying PETG-CF's greater flexibility and susceptibility to permanent deformation compared to PLA.

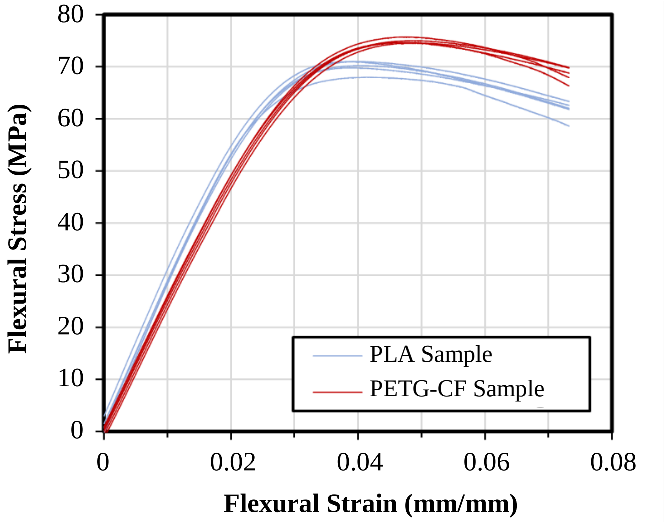

Fig. 6. Flexural stress and flexural strain curve

Table 2: Flexural property of PLA and PETG-CF samples

Mechanical Property	PLA Sample					
	1	2	3	4	5	Avg.
Ultimate Flexural Stress (MPa)	70.98	69.80	67.97	70.22	70.98	69.99
Young's Modulus of Elastic (MPa)	2583.67	2669.52	2605.13	2583.67	2583.67	2605.13
	PETG-CF Sample					
	1	2	3	4	5	Avg.
Ultimate Flexural Stress (MPa)	74.65	74.53	75.00	74.70	75.71	74.92
Young's Modulus of Elastic (MPa)	2415.11	2406.80	2423.17	2423.17	2439.06	2421.46

3.2 AFO Heel Support Bending Test

The heel support model was compressed up to a distance of 45 mm, with two separate tests conducted. In the case of PLA, the first sample fractured but held together, while the second sample completely separated. For PETG-CF, there was more elongation before fracture, but once fracture occurred, immediate separation took place. Fig. 7. Depicts the load-displacement relationship during these tests. The maximum load for both materials, from both compression tests, indicates that PLA has a slightly higher value, as shown in Table 3.

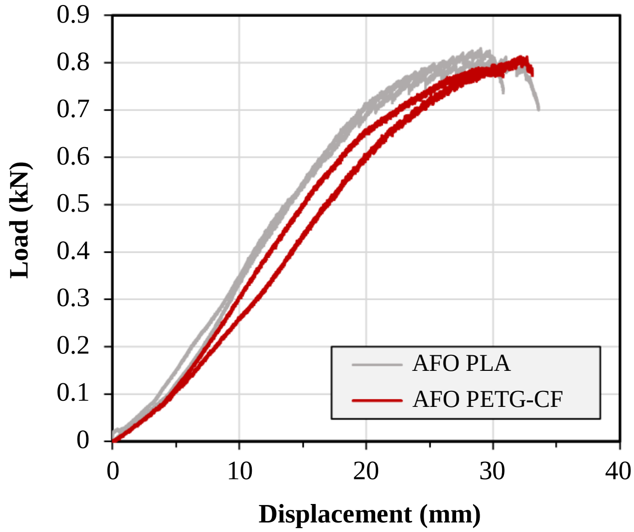

Fig. 7. Load and displacement curve

Table 3: Property of PLA and PETG-CF AFO samples

Property	AFO heel support material					
	PLA			PETG-CF		
	1	2	Avg.	1	2	Avg.
Maximum load (kN)	0.812	0.830	0.821	0.790	0.813	0.801

4. Conclusion

Three-point bending tests were conducted to compare the material properties of PETG-CF and PLA.PETG-CF exhibited 7% increase in ultimate flexural stress compared to PLA, while having a lower Young's modulus of elasticity. This demonstrates PETG-CF's superior strength and flexibility, consistent with the results of heel support tests showing greater displacement compared to PLA. It is evident that PLA has lower strength compared to PETG-CF and a higher Young's modulus. PLA exhibits greater flexibility than PETG-CF, making it less suitable for applications requiring high strength and impact resistance. Despite its higher flexibility, PLA maintains environmental stability and biodegradability, offering an advantage in terms of eco-friendliness over PETG-CF. PETG-CF, on the other hand, excels in durability and resistance to environmental conditions, making it preferable for applications requiring toughness and resilience. The strength improvement offered by PETG-CF could be beneficial in real-world applications where strength and flexibility are both important, such as in the design of AFOs.

Future research can build upon these findings to design AFOs that address both strength and flexibility requirements, offering improved solutions for patients.

References

[1] International Committee of the Red Cross. Manufacturing guidelines: ankle-foot orthosis. Geneva: ICRC; 2010.

[2] Khaing MS, Samala M, Guerra G, Wisessint A. Design and mechanical testing of an adjustable posterior leaf spring ankle-foot orthosis for patients with drop foot. Prothet Orthot Int. 2024;48(1):39-45.

[3] Jin Y, He Y, Shih A. Process planning for the fuse deposition modeling of ankle-foot-orthoses. Procedia CIRP. 2016;42:760-765.

[4] Hollaway LC. Key issues in the use of fibre reinforced polymer (FRP) composites in the rehabilitation and retrofitting of concrete structures. In: Karbhari VM, Lee LS, editors. Service Life Estimation and Extension of Civil Engineering Structures. Cambridge: Woodhead Publishing; 2011. p. 3-74.

[5] Gregor-Svetec D. Polymers in printing filaments. In: Izdebska-Podsiadły J, editor. Polymers for 3D Printing. Oxford: William Andrew; 2022. p. 155-269.

[6] Gao F, Bedard GG. Effects of materials, reinforcement, and heat treatment on thermoplastic solid ankle-foot orthosis mechanical properties. J Prosthet Orthot. 2013;25(3):143-150.

[7] Ansari AA, Kamil M. Effect of print speed and extrusion temperature on properties of 3D printed PLA using fused deposition modeling process. Mater Today Proc. 2021;45:5462-5468.

[8] Makarian K, Taghvaei M, Tu J, Alvarez NJ, Palmese GR. Design, manufacturing, and elastic analysis of digital light processing 3D printed fiber reinforced sandwich beams with thermosetting polymer matrix. Compos Struct. 2023;318:117108.

[9] Ali MH, Smagulov Z, Otepbergenov T. Finite element analysis of the CFRP-based 3D printed ankle-foot orthosis. Procedia Comput Sci. 2021;179:55-62.

[10] Popescu D, Zapciu A, Amza C, Baciu F, Marinescu R. FDM process parameters influence over the mechanical properties of polymer specimens. Polym Test. 2018;69:157-166.

[11] Krivic G, Slavič J. Simultaneous non-contact identification of the elastic modulus, damping and coefficient of thermal expansion in 3D-printed structures. Polym Test. 2023;125:108131.